

## Low-energy-electron-loss spectroscopy of Ge surfaces\*

R. Ludeke and A. Koma<sup>†</sup>

IBM Thomas J. Watson Research Center, Yorktown Heights, New York 10598

(Received 13 August 1975)

Energy-level schemes of intrinsic surface states of annealed (111)  $8 \times 8$  and (100)  $2 \times 2$  Ge surfaces are deduced from the *d*-core-electron and valence-electron excitation spectra. The results compare favorably with tight-binding calculations of the relaxed surface. Empty dangling bond states are observed at the valence-band edge. Their density is estimated to be  $2 \times 10^{14}/\text{cm}^2$  and  $4 \times 10^{14}/\text{cm}^2$  for the (100) and (111) surfaces, respectively. Oxygen-adsorption experiments indicate two different adsorption sites of approximately equal number, but drastically differing activity. The more active sites are associated with the empty dangling bonds, which become saturated near a third and half monolayers, respectively, for the (100) and (111) surface. The oxygen chemisorbs to form quasimolecular GeO complexes independent of surface orientation. The results qualitatively favor the rumpled surface or Haneman model for the (111)  $8 \times 8$  surface reconstruction and suggest a vacancy model for the (100)  $2 \times 2$  surface.

### I. BACKGROUND

Low-energy-electron-loss spectroscopy (LELS) has recently been successfully used to study intrinsic surface states of Si,<sup>1,2</sup> GaAs,<sup>3,4</sup> and Ge.<sup>3</sup> The technique is the most readily available method of studying the electronic properties of the outermost atomic surface layers ( $\sim 5 \text{ \AA}$  for primary energies of  $\lesssim 100 \text{ eV}$ ) and contrast ultraviolet photoemission spectroscopy (UPS) in that both filled and empty electronic states are readily probed, although at reduced resolution. Assignment of structures to surface effects in both UPS and LELS has generally been based on the disappearance of these upon adsorption of foreign atoms such as oxygen or hydrogen. A more convincing proof of the surface origin of some of the structure in LELS for binary semiconductors is the observed changes with composition of the outer surface layer of polar faces by an *in situ* evaporation process, as was reported earlier.<sup>3</sup> However, for the elemental semiconductors one must still rely on surface perturbations by either foreign atoms or by crystallographic changes through surface reconstructions or different surface orientations.

The scattering process in LELS is generally assumed to be a two-step event involving an elastic and an inelastic step or loss event. The elastic event, which may or may not precede the inelastic one, involves the turning around of the incident electron, the momentum being provided by either the crystal lattice (Bragg reflection) or by short-wavelength phonon scattering.<sup>5</sup> This latter process, which causes the thermal diffuse background observed in low-energy-electron diffraction (LEED), is in reality only quasielastic as it involves energy changes of about  $\pm 50 \text{ meV}$ , values small in comparison to the energy resolution of about  $0.5 \text{ eV}$  of conventional detectors employed in LELS.

Theoretical models describing the low-energy-electron-loss process have generally been based on small-angle scattering from the specular or Bragg diffracted beams.<sup>6-8</sup> Both Lucas and Sunjic's semiclassical<sup>6</sup> and Mills' quantum mechanical<sup>8</sup> treatment predict a scattering cross section near the specularly reflected beam proportional to the surface loss function  $-\text{Im}[1/\{\epsilon(\omega) + 1\}]$ , where  $\epsilon(\omega)$  is the energy-dependent dielectric constant of the medium. However, with the exception of Froitzheim and Ibach's work,<sup>9</sup> results of LELS reported in the literature were obtained with electron detectors with broad acceptance angles, such as the hemispherical grid and cylindrical mirror analyzers. Electrons detected by these analyzers have been scattered through large angles and consequently one might expect considerable discrepancies between the theoretical models and experimental results. In fact, for the LELS data presented here, a description in terms of the volume loss function  $-\text{Im}[1/\epsilon(\omega)]$  determined from optical data is in better agreement with experimental data than is the surface loss function.

In this paper the energy-loss spectra of clean (100) and (111) germanium surfaces will be presented in terms of bulk and surface losses. Evidence of surface states is enhanced, and their characterization improved, by analysis of the loss spectra arising from the excitation of electrons from the narrow *d*-core states.<sup>3,4</sup> We furthermore examine the effects of the adsorption of foreign impurities on the strength and energy location of surface-related features in the loss spectrum. We conclude that the so-called "dangling-bond" surface states for both (100) and (111) surfaces are located near the top of the valence band.

### II. EXPERIMENTAL DETAILS

The Ge crystals were cut to the desired orientation, lapped, and chemically polished on pellow

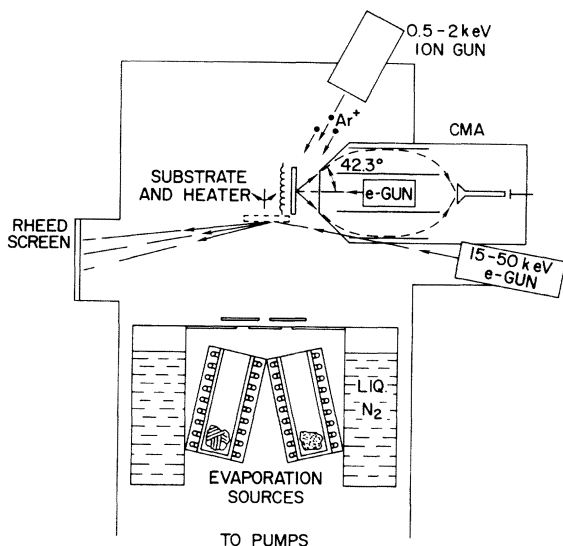


FIG. 1. Experimental apparatus. Sample is shown in the analysis position with primary electron beam of cylindrical mirror analyzer (CMA) normal to surface.

in a dilute sodium hypochlorite solution.<sup>10</sup> Several mils of material were removed, leaving a damage-free and highly polished surface that showed no detail at a magnification of 700 $\times$  in an interference contrast microscope. Prior to mounting the wafer into the ultrahigh vacuum system, it was chemically polished in a dilute CP-4 (HF:CH<sub>3</sub>COOH:HNO<sub>3</sub>:Br in the approximate ratio of 50:500:80:1) solution for approximately one minute. Except as otherwise indicated, both the (111) and (100) oriented crystals were cut from the same undoped ingot, with an electron density of  $7 \times 10^{23}/\text{cm}^3$ .

A schematic of the UHV system is shown in Fig. 1. It incorporates an evaporation stage that is surrounded by a liquid nitrogen cooled shroud and a reflection high-energy electron diffraction (RHEED) system for the determination of the crystallographic condition of the surface. For further analysis the sample is rotated in front of a single-pass cylindrical mirror analyzer with coaxial electron gun (PHI Model 10-150) for Auger electron spectroscopy (AES) and LELS at normal incidence. The sample may be cleaned simultaneously by Ar-ion bombardment.

In a typical operating sequence, an overnight bakeout of the ultrahigh vacuum system reduced the pressure into the low  $10^{-10}$ -Torr range. An Auger spectrum was then taken, which always revealed heavy carbon and oxygen contamination that could only be removed by argon ion bombardment. The substrate was then annealed at temperatures around 500  $^{\circ}\text{C}$ , and the crystallographic condition of the surface simultaneously monitored by RHEED.

The diffraction pattern changed from a diffuse pattern, indicative of an amorphous surface layer, to a detailed, streaked pattern that readily indicated high crystalline perfection with ordered surface reconstructions. The sample was then ready for either thin film overgrowths or surface analysis. Carbon contamination would reappear over a period of hours, with noticeable effects on the LELS spectra, which necessitated additional cleaning and annealing cycles.

The operating conditions for AES and LELS are nearly the same, with the exception that, for the latter, lower primary electron energies are used and that the second harmonic of the modulating voltage of the analyzer is detected to obtain the second-derivative spectra. These spectra are preferable over those in the first derivative, as generally employed in AES, because they allow a more accurate determination of the position of loss structure on the energy scale, although at the price of a lower second-harmonic signal, which varies as the square of the modulation voltage. The choice of primary beam energy is a compromise among resolution, signal intensity and surface sensitivity. The manufacturers indicated resolution of the analyzer is 0.6% of the pass energy for a well focused primary beam. However, the practical limit is set by the thermal spread of the primary electron beam, or approximately 0.4 eV, and by the amplitude of the modulation voltage which for intensity reasons is seldom less than 0.5 V peak to peak. The primary beam current, and hence the signal intensity is nearly linearly related to the primary beam energy below 200 eV, whereas the surface sensitivity is inversely proportional to the energy, with maximum sensitivity near 50 eV. For these reasons, the primary energies and modulation voltages were generally limited to the ranges of 50–100 eV and 0.5–0.8 V peak to peak, respectively. The estimated accuracy in determining the loss structure is  $\pm 0.2$  eV, with somewhat improved precision for averaged values quoted here.

### III. RESULTS

#### A. Clean surfaces

The RHEED patterns of the Ar<sup>+</sup> ion cleaved and annealed Ge (100) and (111) surfaces exhibited clear (2 $\times$ 2) surface reconstructions for the  $\langle 110 \rangle$  azimuths. However, additional diffraction streaks for the [112] azimuth of the (111) surface indicate that the reconstruction for this surface is (8 $\times$ 8).<sup>11</sup> Both (111) 2 $\times$ 2 (Ref. 12) and (111) 8 $\times$ 8 (Ref. 13) structures have been observed by LEED. The latter has since been observed by other workers and has been interpreted as resulting from a (2 $\times$ 8) surface structure that is randomly multipositioned about the three equivalent  $\langle 110 \rangle$  directions.<sup>14</sup>

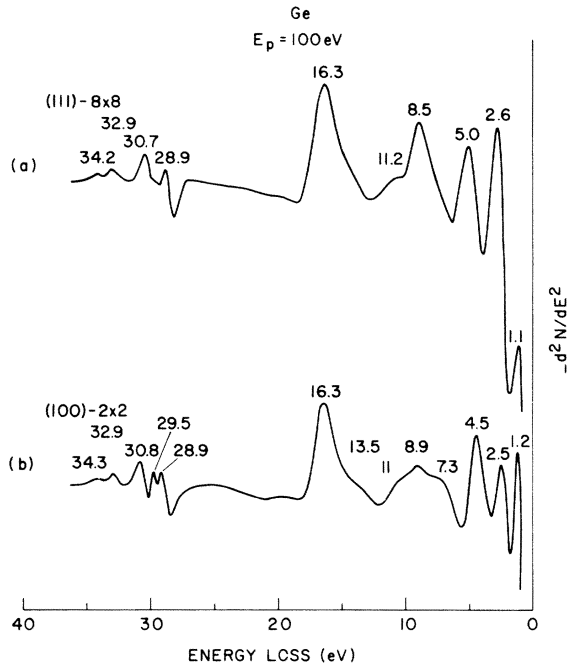


FIG. 2. Second derivative of the energy-loss spectra of the clean and annealed germanium (111)  $8 \times 8$  and (100)  $2 \times 2$  surfaces. Primary electron energy  $E_p = 100$  eV.

The situation for the (100) surface is also not entirely clear, and the possibility of either a  $(2 \times 2)$  or  $(4 \times 4)$  surface reconstruction has been raised.<sup>11,13</sup> Since we do not see any extraneous diffraction streaks other than the  $\frac{1}{2}$  order, we feel that our surfaces are best described as (100)  $2 \times 2$ . It is of interest to note that when the (111) surface was heated to about  $600^\circ\text{C}$  the fractional order diffraction streaks weakened and essentially disappeared, but were recovered upon cooling. Such reappearance was also observed near  $200^\circ\text{C}$  upon cooling a germanium film epitaxially deposited at  $600^\circ\text{C}$  on a (111) substrate. During growth the film surface exhibited a  $(1 \times 1)$  structure. For the (100) surface, on the other hand, the  $(2 \times 2)$  surface structure was observed at elevated temperatures, as well as during epitaxial deposition at  $550^\circ\text{C}$ . Based on these observations alone, there seems to be a basic difference in the nature of the reconstruction on the two surfaces, a point which will be further discussed later in this article.

The energy-loss spectra for the clean (111)  $8 \times 8$  and (100)  $2 \times 2$  surfaces, taken with a primary electron energy of 100 eV, are shown in Fig. 2. Features common to both spectra may be considered of bulk origin. Thus the structure near 2.6 and 4.5 eV is attributed to interband transitions, with energies differing somewhat from optical data.<sup>15,16</sup> The prominent peak at 16.3 eV corresponds to bulk plasmon excitations; whereas the weaker

structure around 11 eV is believed to arise from excitations of surface plasmons, as this number is close to the theoretically expected value of 11.5 eV ( $=\hbar\omega_p/\sqrt{2}$ ). The remaining structure below the bulk plasmon peak is due to surface effects. Although the peak near 1.2 eV is observed on both surfaces, it is definitely not a bulk related structure because its strength is too large compared to the expected bulk value at that energy and because of its great sensitivity to surface cleanliness.

The location of structure on the energy scale does not change with primary electron energy, and it is concluded that diffractive effects, such as those observed for Ni,<sup>17</sup> do not have to be considered here. However, the relative contributions of bulk and surface effects do change with energy, the latter diminishing with increasing energy, in a manner analogous to that observed for GaAs.<sup>4</sup> The intensity of both the volume and surface plasmon peaks increases rapidly with energy so that above 500 eV they completely dominate the loss spectrum. At these energies multipasmon losses also become important, particularly the dual volume plasmon loss around 33 eV. The structure at 32.9 eV observed in Fig. 2 is not of such origin since the multipasmon loss structure is very broad ( $\sim 10$  eV) and is not observed at comparable primary energies in GaAs,<sup>4</sup> where a possibly competing loss mechanism does not exist.

The loss structure in the 29–34 eV range is believed to arise from excitation of  $d$ -core electrons into empty bulk and surface states, as it is well known that the binding energy of the  $d$ -electrons in Ge is around 29 eV.<sup>18</sup> Since the entire loss structure is “tied” to the primary electron energy, there is no other loss mechanism that would explain its origin. The structures at 28.9 eV for the (111) surface and the doublet at 28.9 eV and 29.5 eV for the (100) surface are attributed to transitions into empty surface states, the so-called dangling bond states.<sup>3</sup> The doublet for the (100) surface does not imply two different surface states, but originates from the spin-orbit splitting of the  $d$ -core level. The fact that this splitting has been observed on the (100) surface and not on the (111) surface has been interpreted in terms of differences in symmetry of the dangling bond states for the two surfaces.<sup>19</sup> The remaining three peaks at higher energies arise from excitations into the bulk conduction band.

We have summarized the results of the loss measurements in Table I which also shows relevant data obtained by other experiments.

#### B. Oxygen covered surfaces

We have measured the room temperature uptake of oxygen on clean (111) and (100) surfaces. The results are shown in Fig. 3. The relative increase

TABLE I. Summary of spectroscopic information by LELS for the Ge (111)  $8 \times 8$  and (100)  $2 \times 2$  surfaces and comparison with previous loss and optical data. All energies in eV.

Present LELS structure		Previous ELS	Optical	$-\text{Im}(1/\epsilon)$	Assignment <sup>f</sup>
(111) $8 \times 8$	(100) $2 \times 2$				
1.1	...				ss to ss <sup>g</sup>
...	1.2				bb to ss
2.6	2.5	2.6 <sup>a</sup>	2.35 <sup>c</sup>	2.6 <sup>e</sup>	vb to cb
5.0	4.5	5.0, <sup>a</sup> 5.2 <sup>b</sup>	4.2 <sup>c</sup>	5.3 <sup>e</sup>	vb to cb
...	7.3				bb to ss
8.5	8.9				bb to ss
11.2	11	11.2 <sup>b</sup>		10.5 <sup>e</sup>	surface plasmon
13.5	13.5				bb to ss
16.3	16.3	16.0, <sup>a</sup> 16.4 <sup>b</sup>		16.4 <sup>e</sup>	volume plasmon
28.9	28.9				<i>d</i> core to ss
...	29.5				<i>d</i> core to ss
30.7	30.8	31.7 <sup>b</sup>	32.2 <sup>d</sup>		<i>d</i> core to cb
32.9	32.9				<i>d</i> core to cb
34.2	34.3				<i>d</i> core to cb

<sup>a</sup>50 keV transmission through polycrystalline film, Ref. 20.

<sup>b</sup>200 eV reflection from polycrystalline film, Ref. 21.

<sup>c</sup>Reference 16.

<sup>d</sup>Transmission through polycrystalline film, Ref. 22.

<sup>e</sup>Obtained from Fig. 8.

<sup>f</sup>bb—surface back bond; ss—surface state (dangling bond); vb—valence band; cb—conduction band.

<sup>g</sup>See text for further clarifications.

in the oxygen coverage was monitored by the ratio of the oxygen 510 eV to the germanium 1147 eV Auger lines. This ratio is expected to be a reasonably linear function of the coverage up to about a monolayer of oxygen.<sup>23</sup> The results shown represent the compilation of several adsorption experiments with oxygen pressures ranging from  $2 \times 10^{-8}$  to  $4 \times 10^{-3}$  Torr. For dosages less than about  $0.5 \times 10^{-4}$  Torr min no obvious electron beam effects were observed on the adsorption rates. At substantially higher dosages, particularly in the saturation region, electron beam desorption effects were observed and the beam was always turned off between Auger measurements. These were generally made on previously nonirradiated areas of the sample.

Although the initial uptake is different for the two surfaces, the saturation values of the Auger ratios are nearly the same. Based on atomic densities of the ideal surfaces, and assuming identical adsorption complexes, one would expect a 16% larger signal for the (111) surface than for the (100) surface, whereas only a 3% difference is observed. These differences cannot be reconciled by experimental inaccuracies, but suggest basic topographical differences between the two surfaces.

Previous oxygen adsorption experiments indicate a reasonably fast adsorption process, that tends to saturate near a monolayer of coverage, which is followed by a much slower uptake.<sup>24-27</sup> Our mea-

sured dosages of about  $10^{-2}$  Torr min, required to saturate the oxygen uptake, agree well with previously reported values of  $1-5 \times 10^{-2}$  Torr min.<sup>25,27,28</sup> We will assume here that the observed saturation ratios of 0.65 and 0.63 correspond to monolayer coverages on the (111) and (100) surfaces, respectively.

Further insights into the adsorption process may be obtained from the variation of the sticking coefficient  $S$  with coverage  $\theta$ , expressed as a fraction of a monolayer. These two quantities are related through the equation<sup>29</sup>

$$S = \frac{(N_0/\nu) d\theta}{d(pt)}$$

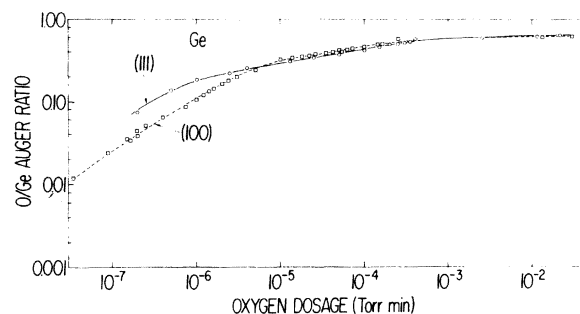


FIG. 3. Normalized oxygen Auger signal as a function of dosage for the (111) and (100) surfaces. Primary electron energy 3 keV; modulation 6 V peak to peak.

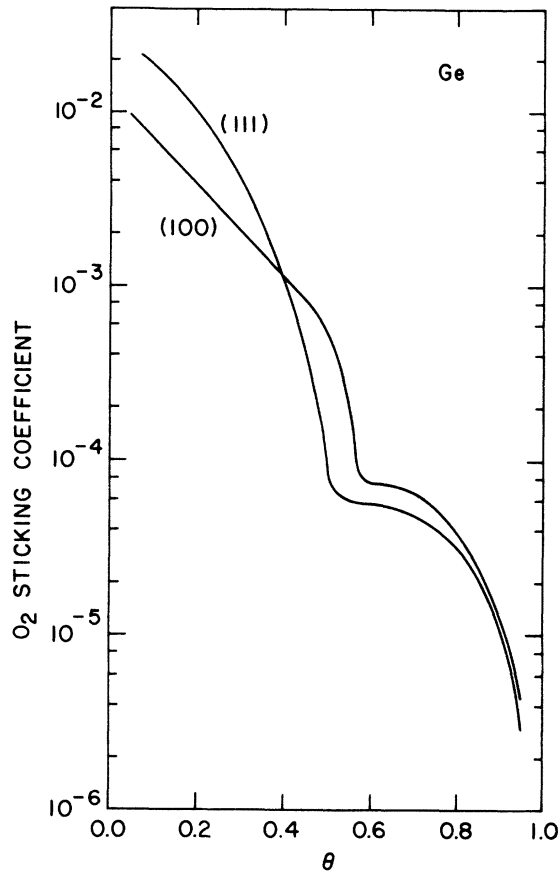


FIG. 4. Sticking coefficient of oxygen as a function of its coverage  $\theta$ , expressed in monolayers, for the (111) and (100) surfaces.

where  $N_0$  is the density of adsorption sites, here the atomic surface density;  $\nu$  is the molecular impingement frequency ( $2.09 \times 10^{22}$  molecules/cm<sup>2</sup> Torr min.); and  $pt$  the dosage in Torr min. The resulting dependence of the sticking coefficient on  $\theta$ , based on the data of Fig. 3, is shown in Fig. 4. The data clearly show a composite adsorption process, indicative of two different adsorption sites of approximately equal numbers but drastically differing activity. The more active sites saturated at  $\theta \sim 0.5$  and  $\theta \sim 0.58$  for the (111) and (100) surfaces, respectively. Monolayer coverage is subsequently achieved after the remaining less active sites have been saturated. Similar behavior of the sticking coefficient near  $\theta = 0.5$  has also been reported for oxygen adsorption on Ge (111) surfaces<sup>28</sup> at 600 °K. Furthermore, a rapid decrease in the heat of adsorption near  $\theta = 0.4$  has been observed for room-temperature adsorption on polycrystalline germanium films.<sup>28</sup> These results strongly suggest the presence of two different adsorption sites. Further discussion will be postponed until after the presentation of energy-loss and electron-

diffraction results. The initial sticking coefficient of  $1.4 \times 10^{-3}$  for the (100) surface is in good agreement with previously reported values<sup>30</sup>; however, considerable discrepancies exist for the (111) surfaces, for which values an order of magnitude smaller than ours have been quoted.<sup>28,30</sup>

The effect of oxygen adsorption on the loss spectra of the Ge (111)  $8 \times 8$  surface is shown in Fig. 5. The spectrum of the clean surface at a primary energy of 70 eV is shown in Fig. 5(a). It is worth noting here that at this energy the surface related structures are more pronounced relative to the bulk related structure than for higher primary electron energies [Fig. 2(a)]. All of the structure is, however, extremely sensitive to oxygen contamination, as seen in Fig. 5(b) for a coverage  $\theta \sim 0.4$ . The surface states have nearly disappeared and new structures appear at 6.8, 30.4, and 31.0 eV. In fact, all evidence of the dangling bond surface states, namely, the 1.1, 28.9, and 29.5 eV peaks, disappears at half a monolayer of oxygen coverage. In addition there are more subtle changes, particularly the shifting and narrowing of the 4.7 eV bulk peak and a relative decrease in intensity of the bulk plasmon peak. The changes become further pronounced upon reaching a mono-

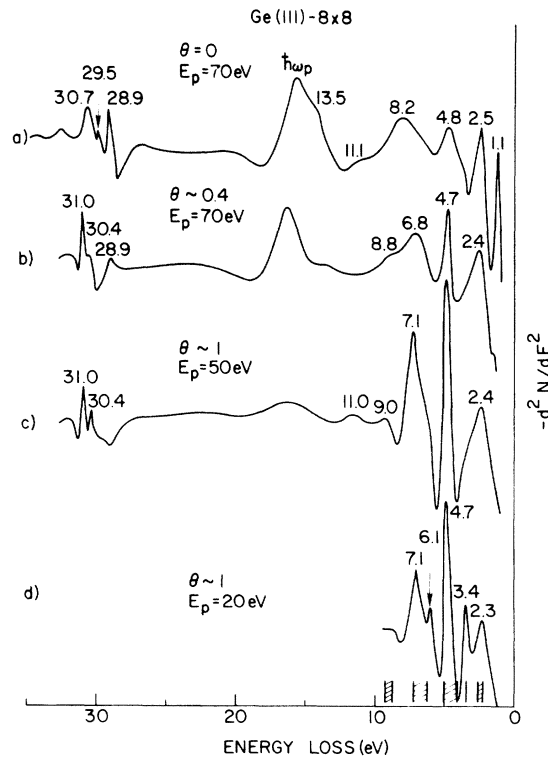


FIG. 5. Energy-loss spectra of the (111) surface for various degrees of oxygen coverage, and for several different primary electron energies. The hatched areas above the abscissa indicate the location of absorption and emission bands for molecular GeO.

layer coverage, as shown in Fig. 5(c). Additional detail is brought out in going to lower primary electron energies, as shown in Fig. 5(d).

The situation for the (100)  $2 \times 2$  surface is nearly identical, with the notable exception that the  $d$  core to surface state transitions already disappear at about a third of a monolayer of adsorbed oxygen. The effect of oxygen on the loss spectra of this surface is shown in Fig. 6. Once again, upon fractional coverage, the surface related structures of the clean surface have essentially disappeared and characteristic peaks at 4.7 and 6.7 eV have emerged [Fig. 6(b)]. Only minor changes occur upon further coverage [Fig. 6(c)]. Thus the loss structure of oxygen on both the (100) and (111) surfaces seems to be characterized by three dominant peaks near 2.5, 4.7, and 6.7 eV. Their relatively narrow line shapes suggest a localized or quasi-molecular description of the oxygen-germanium surface complex. That the 2.5-eV peak is predominantly oxygen derived, rather than bulk related, becomes apparent upon using lower primary electron energies [Figs. 6(e) and 6(f)]. At such energies, bulk contributions for even the clean surface are not resolved within the sensitivity of our instrument.<sup>31</sup>

All of the numbered peaks in Figs. 6(c) and 6(d) have been found to coincide in energy with optical absorption bands of molecular GeO,<sup>32</sup> including the peak at 3.4 eV observed on both surfaces only for low primary electron energies. In molecular GeO, an emission band at this energy corresponds to an optically forbidden triplet transition. Such transitions become possible in inelastic electron scattering because of a breakdown in the first Born approximation at low primary electron energies.<sup>33</sup> Based on these spectroscopic observations, as well as on bond-energy arguments, it was concluded that oxygen chemisorbs on germanium as quasimolecular GeO, with an oxygen atom double-bonded to a germanium surface atom.<sup>32</sup>

#### IV. DISCUSSION

##### A. Clean surfaces

A problem in any spectroscopic identification is the translation of the observed spectra into an energy level scheme that is consistent with experimental results. A knowledge of the possible number of final states is essential, although the number of initially filled states, information potentially obtainable from photoemission spectroscopy, is helpful. Theoretical guidelines may also be helpful; however, calculations for reconstructed surfaces are generally lacking. Nevertheless, based on the unreconstructed Si or Ge surface, one may expect at least four surface related bands: an upper, dangling bond derived band in the vicinity

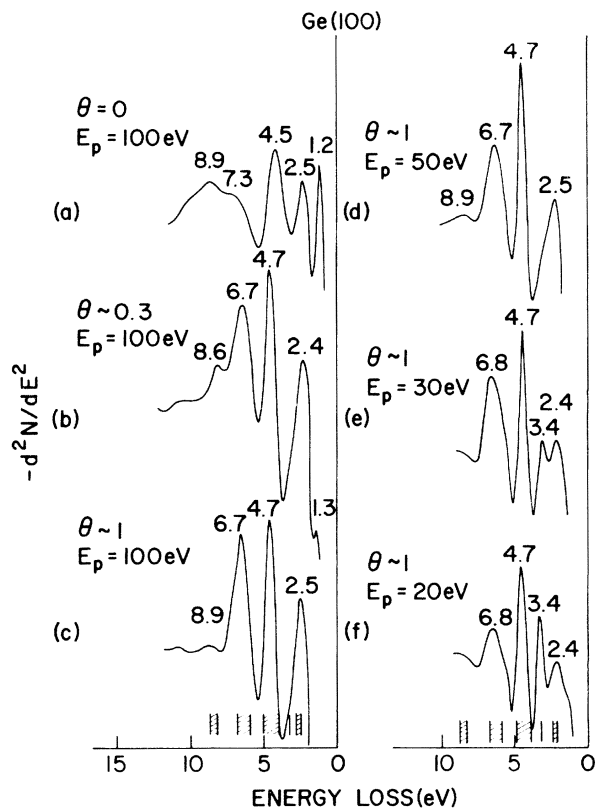


FIG. 6. Effect of oxygen on the energy-loss spectra of the (100) surface.

of the top of the bulk valence band and three lower-lying bands, the so-called back bonds, attributed to the rearrangement of the bonding charge between the surface and subsurface atomic layers.<sup>34,35</sup> Hence, at least three initial states are to be expected, or possibly more, depending on whether the dangling bond states lie partially or completely below the Fermi level and/or if surface reconstruction results in any further splittings of the bands.

Information on the possible final states for surface and bulk transitions is obtainable from the loss spectra involving excitations out of core levels. Since these are energetically sharp and well defined, the resulting spectra need no deconvolution and may be interpreted directly in terms of the density of final states.<sup>3,4</sup> The portion of the  $d$ -core excitation spectrum attributed to bulk effects is plotted with a dashed and dotted line in Fig. 7, assuming a  $d$ -core electron binding energy of 29.3 eV relative to the valence band edge.<sup>36</sup> The over-all features of this curve are in excellent agreement with those expected for the conduction band density of states based on a non-local pseudopotential model.<sup>37</sup>

The assumption that a conduction band state may also be a final state for surface related tran-

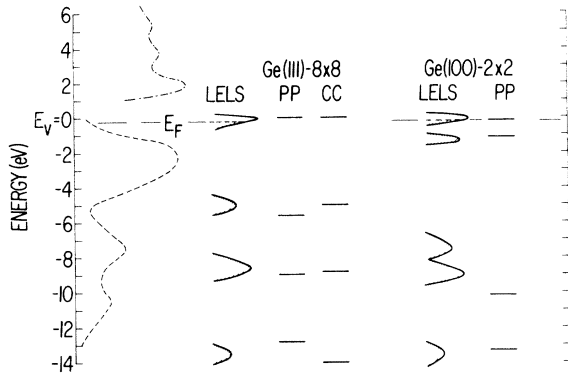


FIG. 7. Energy level schemes of bulk and surface states of the (111)  $8 \times 8$  and (100)  $2 \times 2$  surfaces deduced from energy-loss spectra. PP and CC refer to theoretical tight-binding calculations of Refs. 35 and 38, respectively.

sitions has been proposed for silicon.<sup>1</sup> However, for germanium a potential final state is the empty, dangling bond state observed in the  $d$ -core excitation spectrum. Because of the localized nature of the surface bands,<sup>35</sup> it is likely that the predominant contributions of the surface related structures in the loss spectra involve transitions into the empty dangling bond state. Based on this assumption we have plotted in Fig. 7 the location of the back-bond surface states for the (111)  $8 \times 8$  and (100)  $2 \times 2$  surfaces. The position of the empty dangling bond state at  $0.2 \pm 0.2$  eV below the valence band edge is based on the reported binding energy of  $29.1 \pm 0.1$  eV of the  $d(j = \frac{5}{2})$  core level,<sup>36</sup> since the loss peaks at 28.9 eV in Fig. 2 correspond to excitations from this level. These results imply that the surface is degenerate, as indicated by the position of the Fermi level in Fig. 7. The back-bonding level near  $-5$  eV for the Ge (111)  $8 \times 8$  surface in Fig. 7 is not clearly deducible from the loss spectrum of Fig. 2(a). However, the higher location in energy of the bulk related 5-eV peak in the loss spectrum of the (111) surface, compared to the 4.5 eV value for the (100) surface, is probably due to the presence of a surface state transition. That a surface state should be located in this energy range for the (111) surface is suggested by theoretical tight-binding calculations for the relaxed but unreconstructed (111) surface.<sup>35,38</sup> Based on Pandey and Phillips's (PP) band calculation,<sup>35</sup> we have indicated in Fig. 7 the location of the minima of the surface state bands for both the (111) and (100) surfaces. The step-function densities of states of these minima lie below their parent bulk bands and are expected to contribute strongly to the excitation spectrum. As can be noted, the agreement between their theoretical predictions and our experimental re-

sults is generally very satisfactory, excepting the discrepancies between the middle back bonds of the (100) surface. This agreement furthermore suggests that the assumption of a single final state associated with the empty dangling bond is reasonable and may be quite general in view of similar conclusions for GaAs.<sup>39</sup>

Chadi and Cohen's (CC) calculations<sup>38</sup> for the relaxed (111) surface place the dangling bond surface state by more than one electron volt above the valence band edge, a position which disagrees with present experimental and with Pandey and Phillips' results. However, by aligning Fermi levels, as was done in Fig. 7, the agreement between peaks in their local density of surface states and our experimental, as well as Pandey and Phillips' theoretical results, is substantially improved. For the unreconstructed Ge (111) surface, Chadi and Cohen obtain a more realistic position of 0.5 eV above the valence band edge for the dangling bond state; however, their density of surface states exhibits only one prominent peak, 8 eV below the band edge, which arises from the back bonds.

The loss peak near 1.1 eV for the (111)  $8 \times 8$  surface is probably not a back bond to dangling bond transition, as for the (100)  $2 \times 2$  surface. The intensity of this peak was observed to be strongly dependent upon sample doping<sup>39</sup>: For an  $n$ -type doping level of  $3 \times 10^{18}$  electrons/cm<sup>3</sup>, it completely dominated the loss spectrum, whereas for comparable  $p$ -type doping it was barely observable. We have previously interpreted this peak as arising from excitations of electrons from the filled portion of the dangling bond states to empty surface states lying near the bottom of the bulk conduction band.<sup>39</sup> It is possible that these states arise from a splitting of the dangling bond band because of surface reconstruction. The theoretically predicted width of this band for the unreconstructed surface is 1 eV.<sup>35</sup> The existence of these higher-lying surface states has recently also been postulated by Büchel and Lüth based on surface photovoltage measurements on the (111)  $8 \times 8$  surface.<sup>40</sup>

It is of interest to compare the experimental loss spectra to those predicted by the dielectric model, namely, the bulk loss function  $-\text{Im}[1/\epsilon(\omega)]$  or the surface loss function  $-\text{Im}\{1[\epsilon(\omega) + 1]\}$ . In order to make this comparison, we found it computationally easier to differentiate the loss functions<sup>41</sup> and suitably average it so that a resolution of about 1 eV was obtained. The results are shown in Fig. 8. The primary electron energy (150 eV) was chosen so that in the resulting loss spectrum the ratio of peak heights of the bulk plasmon to bulk interband transitions coincided nearly with the dielectric data. Clearly this over-all agree-

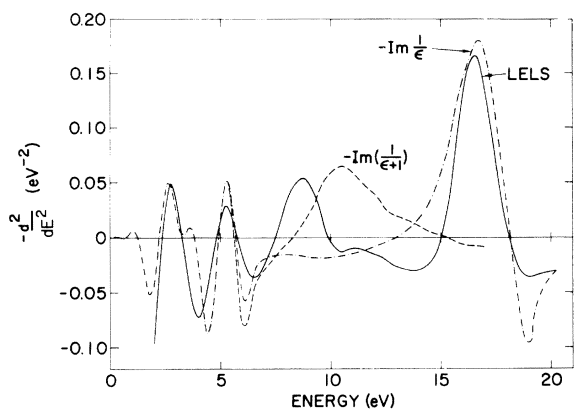


FIG. 8. Comparison of the second derivative of the volume and surface loss functions, calculated from the optical data of Ref. 41, to the experimental energy-loss spectrum of the Ge (111) surface for  $E_p = 150$  eV.

ment is obtainable only for this energy, as particularly the bulk plasmon peak diminished in intensity for lower primary energies.

Since below 6 eV the bulk and surface loss functions are essentially identical, agreement between them and the experimental loss data is very good. However, above this value considerable discrepancies exist between the curves, with the bulk loss function resembling the experimental data better than the surface loss function. The experimental peak near 8.5 eV, attributed to surface states, is of course not obtained from bulk optical data. The experimentally observed surface plasmon peak near 11 eV is rather weak, whereas the dielectric model suggests a much stronger peak at 10.5 eV.

Agreement between the low-energy loss spectra and the bulk<sup>2</sup> and surface loss function<sup>42</sup> have been reported previously. However, the comparison to the surface loss function was made only below 8 eV and therefore does not constitute a sufficient criterion for its validity over the complete spectrum.

#### B. Oxidized surface

The similarities between the loss spectra of the oxidized germanium surfaces and the optical spectra of molecular GeO, as well as the experimental observation that the oxygen desorbs as molecular GeO near 400 °C,<sup>32</sup> strongly suggest that the oxygen is chemisorbed into a bonding state characterized by the germanium-oxygen double bond of GeO. Thus the ideal Ge (100) surface, with its two dangling bonds per surface atom, presents a nearly perfect bonding match to each oxygen atom. The situation for the (111) surface, however, requires that a germanium back bond be broken to satisfy the double bond to the oxygen atom. The chemisorption proceeds by the splitting of the oxygen

molecule, at a cost of 119 kcal/mole, the breaking of surface bonds on the (100) and back bonds on the (111) surface, at a cost of<sup>43</sup> 30 and 45 kcal/bond, respectively, and the formation of the germanium-oxygen double bond with a gain of 161 kcal/mole. The resulting heats of formation of -113 and -173 kcal/mole of O<sub>2</sub> for the (111) and (100) surfaces are thus substantially larger than the -50 kcal/mole expected for the peroxide bridge, and constitute additional support for the Ge=O model.<sup>32</sup>

The possibility that the formation of GeO is beam activated can be dismissed based on room temperature calorimetric studies which reveal a heat of adsorption of -132 kcal/mole on polycrystalline films.<sup>28</sup> This value, which is close to the averaged value of the present estimate for the heats of formation of GeO on the (100) and (111) surfaces, clearly indicates a strongly exothermic process. Since energetically the other possibility is the formation of GeO<sub>2</sub>, which is unlikely for monolayer or submonolayer coverage<sup>44</sup> and which is not observed spectroscopically by LELS, it is concluded that the proposed Ge=O model is the most likely adsorbate complex on germanium. Further support that oxygen chemisorbs at room temperature is obtained from spin-resonance measurements, which indicate that the oxygen resonance line disappears near room temperature—indicating a pairing of the electrons—whereas it is detectable at cryogenic temperatures where oxygen is presumably just physically adsorbed.<sup>45</sup>

The behavior to oxygen exposure of the various surface related features may be used to distinguish and possibly support particular models of the reconstructed surfaces of germanium. Two basic models for surface reconstructions of annealed germanium and silicon surfaces are principally discussed, namely, the vacancy or Lander-Morrison (LM) model<sup>46</sup> and the rumpled surface or Hanemann (H) model.<sup>47</sup> Based on the proposed oxidation model of one oxygen atom per germanium surface atom, one can argue, assuming no further lateral displacements of surface atoms, that the oxygen layer would replicate a surface with vacancies, thereby basically preserving the order of the surface as observed through electron diffraction (either LEED or RHEED). We observe such behavior for the (100) 2×2 surface, but not for the (111) 8×8 surface, for which the fractional order diffraction streaks disappear at a coverage of about half a monolayer. Because of this, as well as difficulties in interpreting LEED data of the (111) 8×8 structure in terms of the LM model,<sup>14</sup> we will attempt to interpret our experimental observations for the (111) surface in terms of the H model.

The basic atomic arrangement of this model is shown in Fig. 9. One-fourth of the surface atoms,



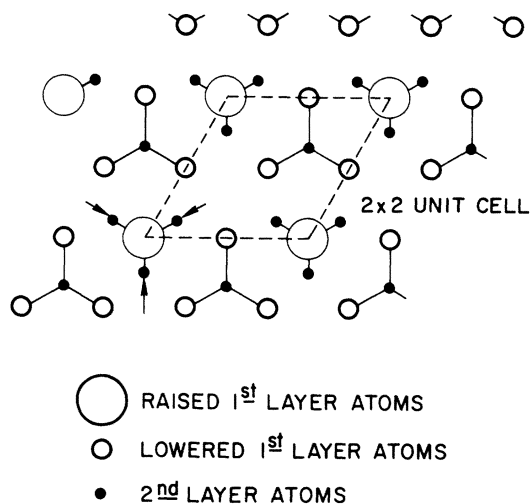


FIG. 9. Haneman model (Ref. 47) for the Ge (111)  $2 \times 2$  surface.

every second atom in alternate rows along an arbitrary [110] direction, is raised above the surface plane, which permits the neighboring atoms of the second layer to move radially towards the raised atoms, as indicated by the arrows in the figure. The resulting geometrical arrangement is no longer tetrahedral, but closer to a trigonal pyramid, for which the bond electron configuration is  $p^3$ . As a result the fourth orbital or dangling bond of the surface atom assumes an  $s$ -like character. The remaining three-fourths of the surface atoms are depressed to form a more planar configuration with the second layer atoms. This arrangement, more appropriately described by an  $sp^2$  orbital configuration, causes the dangling bond orbital to assume a  $p$ -like character and to be chemically more active in the absorption process.<sup>47</sup> The unit cell of this arrangement is  $(2 \times 2)$ ; however, it has been shown that the model can readily be adapted to give a  $(2 \times 8)$  unit cell, which when multipositioned about the three equivalent  $\langle 110 \rangle$  directions can explain the incomplete set of eighth-order diffraction spots.<sup>14</sup>

Our experimental observations of (i) two different absorption sites, (ii) the disappearance of the surface reconstruction and the empty dangling bond states upon fractional oxygen coverage, and (iii) the  $p$ -like character of the dangling bond states,<sup>19</sup> can adequately be described by the H model; An oxygen atom randomly chemisorbed on one of the lowered surface atoms requires the breakage of an additional bond to a second layer atom to form the double-bonded GeO molecule. The affected second layer atoms would tend to interact with the dangling bond of one of the two remaining surface atoms and eliminate it as a

rapid absorption site. The net effect is that the number of rapid adsorption sites is about half the atomic surface density; a number in good agreement with our observations. Each adsorption is accompanied by a local atomic rearrangement. Since this process is random, the resulting disorder explains the disappearance of the surface reconstruction at somewhat less than half a monolayer of adsorbed oxygen.

The situation for the (100)  $2 \times 2$  surface is basically different in that the  $(2 \times 2)$  surface structure disappears neither during epitaxial deposition nor during oxygen adsorption, although the diffraction pattern weakens near monolayer coverage. Although the disappearance of the half-order diffraction streaks near  $10^{-5}$  Torr min exposure has been reported,<sup>11</sup> we repeatedly observed their presence at 50 times greater dosages. For reasons mentioned above, we believe that this evidence supports a vacancy model. The high saturation Auger ratio furthermore suggests that the atomic surface density is comparable to that of the (111) surface or about 16% greater than for the ideal (100) surface. This increase can also be explained by the vacancy model. In fact, the LM model suggests a 50% increase in the number of exposed atoms on the (100) surface through removal of half the atoms in the first layer and a pairing between the remaining atoms and also between second layer atoms. The environment of the paired atoms in the first and second layer is however different and hence suggests different chemical behavior relative to adsorbed foreign atoms. A pairing of the surface atoms and the formation of double bonds may furthermore explain the hybrid  $s-p$  character observed for the dangling bond states.<sup>19</sup> However, it is premature to conclude that the LM model is representative of the Ge (100) surface in view of the rather extreme bond distortions implied by the model and the lack of detailed calculations of the configurational energy relative to the unreconstructed surface, although arguments on an empirical bonding model have been formulated.<sup>48</sup>

It is also possible to estimate the density of empty dangling bond states from the observed fractional coverage of oxygen necessary to saturate them and the knowledge of the one to one correspondence of adsorbed oxygen atoms to germanium surface atoms. Based on the nearly equal oxygen Auger saturation signal to the (100) and (111) surfaces, one may assume a density of surface atoms of  $7.3 \times 10^{14}/\text{cm}^2$ , corresponding to the unreconstructed (111) surface, for both surfaces. The density of dangling bond states is then estimated to be  $2.4 \times 10^{14}/\text{cm}^2$  for the (100)  $2 \times 2$  surface and  $3.6 \times 10^{14}/\text{cm}^2$  for the (111)  $8 \times 8$  surface. These values represent lower limits. An upper limit of  $5.4 \times 10^{14}/\text{cm}^2$  may be estimated for the

(111)  $8 \times 8$  surface by assuming the H-model, as discussed above.

We acknowledge helpful discussions with H. Lüth and L. L. Chang.

\*Research sponsored in part under ARO Contract.

<sup>†</sup>Present address: Dept. of Applied Physics, University of Tokyo, Japan.

<sup>1</sup>J. E. Rowe and H. Ibach, Phys. Rev. Lett. **31**, 102 (1973).

<sup>2</sup>H. Ibach and J. E. Rowe, Phys. Rev. B **9**, 1951 (1974); **10**, 710 (1974).

<sup>3</sup>R. Ludeke and L. Esaki, Phys. Rev. Lett. **33**, 653 (1974).

<sup>4</sup>R. Ludeke and L. Esaki, Surf. Sci. **47**, 132 (1975).

<sup>5</sup>V. Roundy and D. L. Mills, Phys. Rev. B **5**, 1347 (1972).

<sup>6</sup>A. A. Lucas and M. Sunjic, Phys. Rev. Lett. **26**, 229 (1971); and *Progress in Surface Science*, edited by S. G. Davison (Pergamon, Oxford, 1972), Vol. 2., p. 75.

<sup>7</sup>C. B. Duke, in *Electron Emission Spectroscopy, Proceedings of Nato Summer Institute, Ghent, 1972*, edited by W. Dekeyser, L. Fiermans, G. Vanderkelen, and J. Vennik (Reidel, Dordrecht, 1973).

<sup>8</sup>D. L. Mills, Surf. Sci. **48**, 59 (1975).

<sup>9</sup>H. Froitzheim and H. Ibach, Surf. Sci. **47**, 713 (1975).

<sup>10</sup>A. Reisman and R. Rohr, J. Electrochem. Soc. **111**, 1425 (1964).

<sup>11</sup>G. J. Russell, Surf. Sci. **19**, 217 (1970).

<sup>12</sup>J. J. Lander and J. Morrison, J. Appl. Phys. **34**, 1403 (1963).

<sup>13</sup>F. Jona, IBM J. Res. Develop. **9**, 375 (1965).

<sup>14</sup>P. W. Palmberg and W. T. Peria, Surf. Sci. **6**, 57 (1967).

<sup>15</sup>H. Ehrenreich, in *The Optical Properties of Solids*, edited by J. Tauc (Academic, New York, 1966), p. 106.

<sup>16</sup>H. R. Philipp and H. Ehrenreich, Phys. Rev. **129**, 1550 (1963).

<sup>17</sup>E. Sickafus and F. Steinrisser, Phys. Rev. B **6**, 3714 (1972).

<sup>18</sup>J. A. Bearden and A. F. Burr, Rev. Mod. Phys. **39**, 125 (1967).

<sup>19</sup>R. Ludeke and A. Koma, Phys. Rev. Lett. **34**, 817 (1975).

<sup>20</sup>K. Zeppenfeld and H. Raether, Z. Phys. **193**, 471 (1966).

<sup>21</sup>J. Thirwell, Proc. Phys. Soc. Lond. **91**, 552 (1967).

<sup>22</sup>M. Cardona, W. Gudat, B. Sonntag, and P. Y. Yu, *Proceedings of the International Conference on the Physics of Semiconductors, Cambridge, Mass., 1970* (A. E. C., Oak Ridge, Tenn., 1970), p. 209.

<sup>23</sup>An upper estimate of the attenuation may be made by assuming an escape depth for the 1147 eV electron in Ge to be 20 Å [G. Ertl and J. Küppers, in *Low Energy Electrons and Surface Chemistry* (Chemie, Weinheim, 1974)] and an oxide layer thickness of 1.6 Å [R. T. Sanderson, *Chemical Bonds and Bond Energy*, (Academic, New York, 1971)]. Thus  $I \sim e^{-1.6/20} = 0.92$ , which corresponds to an 8% attenuation of the 1147-eV Auger electrons. In reality one may expect the oxygen atoms to be less effective scatterers than the germanium atoms with their substantially greater effective charge, so that the expected attenuation is less than this upper limit.

<sup>24</sup>M. Green, J. A. Kafalas, and P. H. Robinson, *Semi-*

*conductor Surface Physics*, edited by R. H. Kingston (University of Pennsylvania, Philadelphia, Pa., 1957), p. 349.

<sup>25</sup>M. Green and A. Liberman, J. Phys. Chem. Solids **23**, 1407 (1962).

<sup>26</sup>D. Brennan, D. O. Hayward, and B. M. W. Trapnell, J. Phys. Chem. Solids **14**, 117 (1960).

<sup>27</sup>A. H. Boonstra, Philips Res. Rep. Suppl. No. 3 (1968).

<sup>28</sup>A. A. Frantsuzov and N. I. Makrushin, Surf. Sci. **40**, 320 (1973).

<sup>29</sup>D. O. Hayward and B. M. W. Trapnell, *Chemisorption* (Buttersworth, London, 1964).

<sup>30</sup>R. E. Schlier and H. E. Farnsworth, J. Chem. Phys. **30**, 917 (1959).

<sup>31</sup>Aside from a general decrease in signal intensity due to the decreasing primary electron current, a smearing out of bulk features upon lowering the primary electron energy may be expected for two reasons: (a) a modest decrease in the scattering length will emphasize surface contributions, and (b) the contribution of indirect transitions becomes important. This follows from the conditions of conservation of energy and momentum  $\Delta k \approx (\Delta E/K_0 \hbar^2) m_e$ , where for a given energy loss  $\Delta E$ ,  $\Delta k$ —the momentum transferred—increases as the momentum  $K_0$  of the primary electron is lowered.  $\Delta k$  may readily span portions of the Brillouin zone (Ref. 4). Thus for strongly dispersive energy levels, the loss spectrum at low primary energies represents to a large extent an integrated spectrum over momentum space and is nearly featureless unless differential detecting schemes are employed. In contrast, localized excitations are considerably enhanced because of their lack of dispersion in reciprocal space.

<sup>32</sup>R. Ludeke and A. Koma, Phys. Rev. Lett. **34**, 1170 (1975).

<sup>33</sup>N. F. Mott and H. S. W. Massey, *The Theory of Atomic Collisions*, 3rd ed. (Clarendon, Oxford, 1965).

<sup>34</sup>J. A. Appelbaum and D. R. Hamann, Phys. Rev. Lett. **31**, 106 (1973); **32**, 225 (1974).

<sup>35</sup>K. C. Pandey and J. C. Phillips, Phys. Rev. Lett. **32**, 1433 (1974).

<sup>36</sup>D. E. Eastman and J. L. Freeouf, Phys. Rev. Lett. **33**, 1601 (1974). The value of 29.3 eV is a weighted average of the  $d(j=\frac{5}{2}) = 29.1$  eV and  $d(j=\frac{3}{2}) = 29.65$  eV values of the spin-orbit split  $d$ -core levels.

<sup>37</sup>W. D. Grobman, D. E. Eastman, J. L. Freeouf, and J. Shaw, Proceedings of the Twelfth International Conference on the Physics of Semiconductors, Stuttgart, 1974 (unpublished), p. 1275.

<sup>38</sup>D. J. Chadi and M. L. Cohen, Solid State Commun. **16**, 691 (1975).

<sup>39</sup>R. Ludeke and A. Koma, Solid State Sci. **5**, 259 (1975).

<sup>40</sup>M. Büchel and H. Lüth, Surf. Sci. **50**, 451 (1975).

<sup>41</sup>Data calculated from optical constants kindly supplied by H. R. Philipp (see also Ref. 16).

<sup>42</sup>J. E. Rowe, H. Ibach, and H. Froitzheim, Surf. Sci. **48**, 44 (1975); H. Froitzheim, H. Ibach, and D. L. Mills, Phys. Rev. B **11**, 4980 (1975).

<sup>43</sup>This value represents an improved estimate of the expected lowering of the surface energy because of inter-

actions between the pairs of dangling bonds on the (100) surface. M. Green and R. Seiwatz, *J. Chem. Phys.* **37**, 458 (1962).

<sup>44</sup>The formation of tetrahedrally coordinated  $\text{GeO}_2$  requires the oxygen to penetrate into the sublayers and breaking three Ge-Ge bonds per oxygen molecule. Such a process was proposed for the oxidation of silicon by M. Green and K. H. Maxwell [*J. Phys. Chem. Solids* **13**, 145 (1960)] but is unlikely to occur at room temperature (Ref. 32).

<sup>45</sup>J. Higinbotham and D. Haneman, *Surf. Sci.* **34**, 450 (1973).

<sup>46</sup>J. J. Lander and J. Morrison, Ref. 12. Their model assumes a 50% and 25% vacancy in the atomic surface layer of the (100) and (111) surface, respectively.

<sup>47</sup>D. Haneman, *Phys. Rev.* **121**, 1093 (1961); D. Haneman and D. L. Heron, *The Structure and Chemistry of Solid Surfaces*, edited by G. A. Somorjai (Wiley, New York, 1969), p. 24-1.

<sup>48</sup>J. C. Phillips, *Surf. Sci.* **40**, 459 (1973).